Proceedings of the
Annual Stability Conference
Structural Stability Research Council
Louisville, Kentucky, April 13-16, 2021

Numerical investigation of the flexural buckling of high strength steel wide flange columns

M. Farhan Akhtar[1], Rachel A. Chicchi[2]

Abstract

High strength structural steel (HS3) provides a number of economic, environmental, and engineering advantages afforded by reduced member sizes in comparison to conventional steel. This steel is particularly advantageous in strength-controlled conditions, such as in gravity columns. Despite these benefits, engineers and contractors in the US have been reluctant to use this material. This is partially due to cost and availability, but also likely due to the lack of guidance in AISC 360-16 regarding HS3. This study numerically investigates the buckling capacity of concentrically loaded gravity columns with HS3 grades of 550 MPa (80 ksi), 690 MPa (100 ksi), and 890 MPa (130 ksi). Rolled wide flange columns are considered. The numerical modeling was conducted in ABAQUS and was validated against experimental test results present in the literature. After validation, W12×58 and W14×90 columns were evaluated for all three yield strengths with slenderness ratios ranging from 40 to 160. Initial imperfections and residual stresses were incorporated. The buckling capacity of the HS3 columns was compared with conventional steel columns in order to understand the effectiveness of high strength steel. Also, the applicability of the AISC 360-16 design equations for flexural buckling of wide flange columns was evaluated. It was found that the current design equations can predict the ultimate strength of HS3 gravity columns with sufficient accuracy.

1. Introduction

High-strength structural steel (HS3) exhibits higher yield strengths than traditional structural steels (such as ASTM A992 and A36). These higher strengths can be achieved through metallurgical changes (such as high strength low alloy steel, HSLA, or advanced high strength steel, AHSS) and/or through processing such as quenching and tempering or the thermo-mechanical control process (TMCP). This broad category of high strength steels has become more prominent in Asia, Australia, and Europe in recent years (Oakley, 2014). HS3 is classified differently in different areas of the world but it is generally categorized as steel with yield strengths equal to or greater than approximately 65 ksi. In this study, in order to realize the increased potential of using high strength steels, HS3 will refer to low-carbon steel with yield strengths equal to or greater than 550 MPa (80 ksi).

[1] Graduate Research Assistant, University of Cincinnati, <akhtarmn@mail.uc.edu>
[2] Assistant Professor, University of Cincinnati, <chicchrl@ucmail.uc.edu>

The increased yield strength of high strength structural steel (HS3) is beneficial when designing strength-controlled members. If effectively utilized, HS3 can result in smaller shapes, leading to decreased weight, decreased transportation, and decreased fabrication costs. Lighter sections will also reduce the overall weight of the structure, which may result in reduced foundations. However, there are some drawbacks to HS3 that must be acknowledged. HS3 has less ductility as compared to conventional steel, as shown in Fig.1 (Baddoo & Brown, 2015). This can be seen by a shorter strain hardening region with HS3 steel than conventional steel. This reduced ductility restricts its use in seismic applications. Additionally, the modulus of elasticity is not improved with higher strength steels. Thus, HS3 is not advantageous for deflection-controlled members, such as beams, but is ideal for members that experience high axial forces. For example, roof trusses at the Sony Center in Berlin, Germany were composed of solid rectangular sections of 460 MPa (67 ksi) and 690 MPa (100 ksi) (Oakley, 2014). Two International Finance Center in Hong Kong is an 88-story skyscraper that opened in 2003 used six steel-concrete columns composed of 5000 tons of high strength structural steel for the lower 6 levels (Rakshe & Patel, 2010). The United States has been slower to implement HS3 in building construction when compared with its international counterparts.

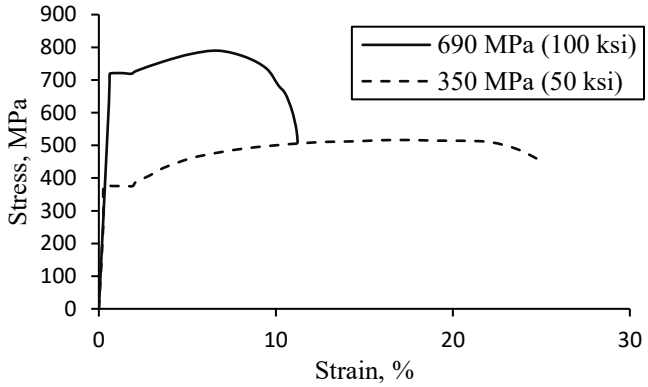

Figure 1: Stress-strain curve of different grades of steel (Baddoo & Brown, 2015).

1.1 Motivation

To promote the use of HS3 in building construction, an American Institute of Steel Construction (AISC) Ad hoc task group was developed to advance the use of high strength steel (AISC Committee on Specification, 2019). This committee of industry professionals and academics served to provide guidance and encourage innovation in the application of HS3. They identified barriers and proposed a path forward for implementation. One necessary step that was identified was compilation and review of new and existing research to justify expansion of yield strength limits for HS3 in the AISC *Specification.* The work presented in this paper aims to support these efforts.

This study will evaluate the applicability of the current gravity column design equations for HS3 design and provide a better understanding of the flexural buckling behavior of HS3 columns through finite element modeling. Concentrically loaded, wide flange gravity columns with yield strengths of 80, 100, and 130 ksi are studied relative to conventional ASTM A992 column behavior. Columns were selected to be studied because of the potential member size reductions that can be achieved when using high strength steel. These benefits would not be as noteworthy in primarily deflection-controlled applications.

1.2 Previous Studies

Most research regarding the buckling behavior of high strength structural steel was conducted in order to evaluate the applicability of international design codes for HS3 with limited focus on the AISC *Specification.* Many of these studies also used built-up box or I-sections instead of rolled shapes. A brief summary of some of this work is provided.

Rasmussen and Hancock (1995) proposed a test program to select a design curve for a 690 MPa (100 ksi) steel column using AS 4100-1990 (1990). They assessed welded box and I-section columns for both eccentric and non-eccentric concentrated axial loads and compared their results with EN 1993-1:1990 (1990), ANSI/AISC 360-1993 (1993), and BS 5950-1:1990 (1990). It was concluded that the Australian, American, and British specifications were in close agreement with the test results. Eurocode design curves were conservative when compared with the test results.

Ma et al. (2018) experimentally investigated the structural behavior of a 690 MPa (100 ksi) slender, welded H-section column under axial loading and compared the results with Chinese GB50017-2003 (2009), Eurocode EN1993-1-1: 2005 (2011), and ANSI/AISC 360-16 (2016). It was found that EN1993-1-1 and GB50017-2003 significantly underestimated the buckling resistance of welded H-sections with 690 MPa (100 ksi) yield strengths. It was reported that ANSI/AISC 360-16 was in close agreement with the measured failure loads.

Ban et al. (2013) investigated the mechanical behavior of 960 MPa (140 ksi) steel columns under axial compression through an experimental program. The study investigated six built-up, welded specimens consisting of both I- and box-sections. Based on the limited experimental results, a comprehensive numerical parametric study was conducted for the same yield strength, considering different slenderness ratios and cross-sectional dimensions. It was reported that all specimens failed by overall buckling and that the current design curves underestimated the buckling capacity of HS3 columns. However, the column curve in both Chinese codes, GB50017-2003 and EN 1993-1:1990 could be used along with the ANSI/AISC 360-10 column curve, to conservatively predict the buckling capacity of these columns. The study also proposed new column curves to calculate the load-carrying capacity of 960 MPa steel columns with sufficient accuracy.

2. Numerical Modeling

ABAQUS (Dassault Systemes, 2014), a commercially available finite element method (FEM) modeling package, was used to determine the load-carrying capacity of HS3 gravity columns subjected to flexural buckling. The four-node doubly-curved shell element with reduced integration (S4R) was used to perform all analyses, as suggested and validated by Agarwal (2011) and Takagi and Deierlein (2007). These shell elements can account for residual stress, inelastic flexural torsional buckling, and local buckling without being as computationally expensive as solid elements. The shell element has 6 degrees of freedom per node and five integration point through the thickness and one reduced integration point along length and width. A mesh convergence study determined that partitioning of the web and flanges each into eight parts was computationally feasible while still predicting results with sufficient accuracy. The column was meshed along its length with the same size as of a partition width of flange and the same size is applied for flange and web along the whole length, as shown in Fig. 2. The figure shows the percent error with respect to (w.r.t.) the column with 12 elements along its web and flange.

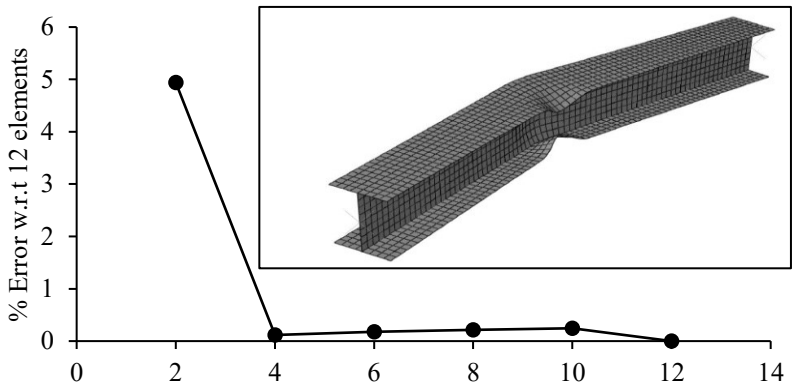

Figure 2: Mesh Convergence

Columns in this study were modelled with pinned and roller supports. The loaded end was modelled as a roller which was free to translate along the column length to allow movement for buckling. The column base was pinned. Linear kinematic constraints were applied at the flanges and web of the column ends to ensure rigid, planar behavior. Axial load was applied to the shape's centroid at the top of the column.

The load-carrying capacity of the column was determined using RIKS analysis, which is generally used to predict the unstable and geometrically non-linear collapse of a structure. Geometric imperfections were incorporated through a linear elastic, eigenvalue buckling analysis performed in ABAQUS. Global and local imperfections, as shown in Fig. 3, were captured. Local imperfections had an amplitude of 1.6 mm (1/16 in.), as per the maximum permitted variation in cross-section by ASTM A6 (2019). The amplitude of the global imperfection was equal to the column length divided by 1000, based on the AISC *Specification* (2016) recommendations for maximum out-of-plane straightness.

The material model used for modeling HS3 was adopted from tensile coupon tests performed by Huang et al. (2018). Tests were performed on HS3 steel with three different yield strengths: 550 MPa (80 ksi), 690 MPa (100 ksi), and 890 MPa (130 ksi). The engineering stress-strain curves for these three material strengths have been reproduced in Fig. 4.

Residual stress was incorporated within the model using fictitious temperatures. This approach is outlined in Agarwal (2011). In general, residual stress in high strength structural steel (HS3) is comparatively less detrimental than conventional steel, but there is no consistency reported in the present literature regarding tensile residual stress (Kim et al., 2014; Uy, 2001; Somodi & Kovesdi, 2018). Considering these factors, a residual stress of 150 MPa (22 ksi) was chosen in order to conservatively accommodate all three material strengths being considered based on the literature. The distribution of residual stress was presumed to be the same as of conventional steel, i.e. equal tensile and compressive residual stresses along with tensile stress at ends of web and at the center of flanges, with compressive stresses at the ends of flanges and at the center of the web. However, conventional steel analyses typically incorporate a residual stress equal to 30% of the yield strength, as recommended in the AISC *Specification* (2016).

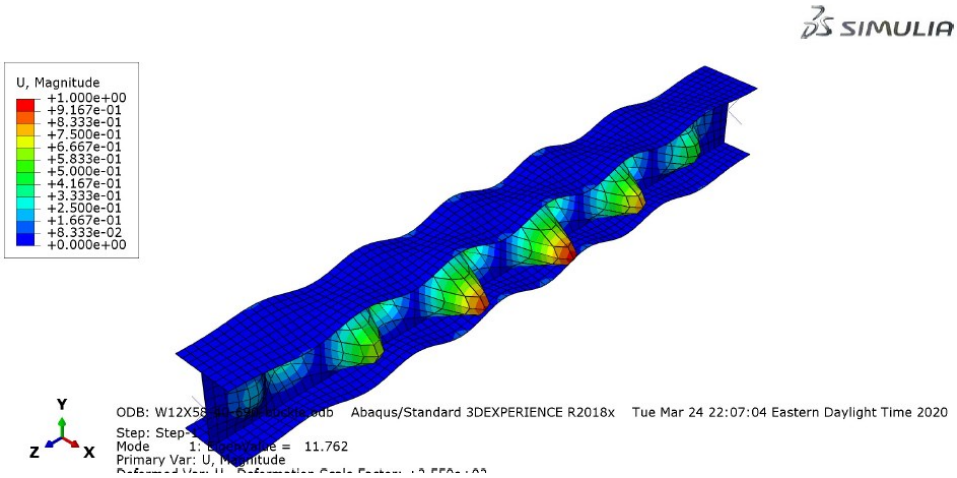

a) Local Imperfections

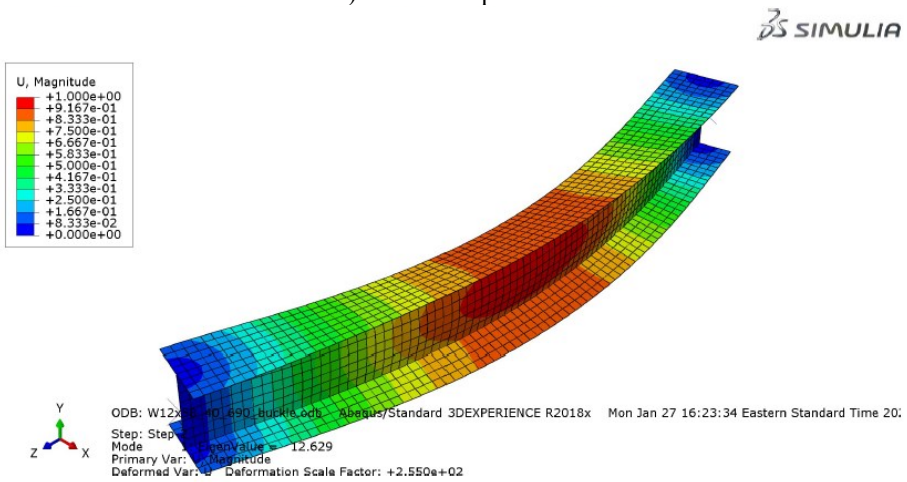

b) Global Imperfections

Figure 3: BUCKLE analysis results showing a) Local and b) Global Geometric Imperfections

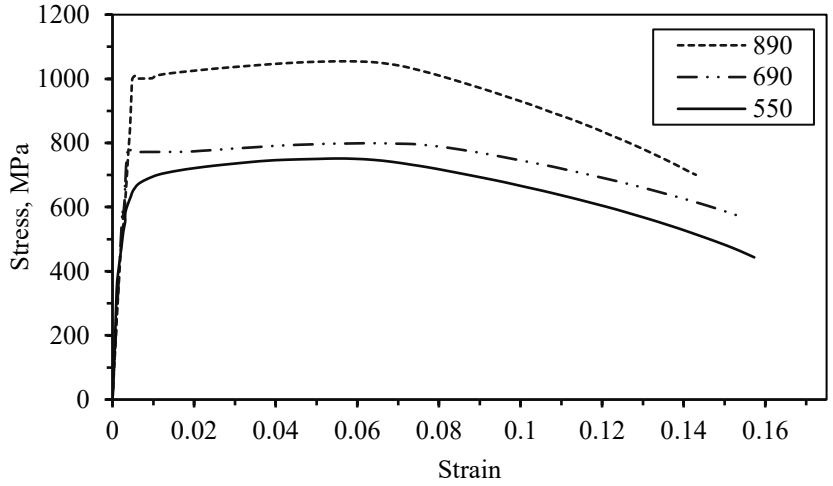

Figure 4: Stress-Strain Curve (Huang et al., 2018)

3. Validation of Numerical Model

The modeling approach used in this study was validated through comparison with the experimental study conducted by Ma et al. (2018) on welded high strength structural steel columns. Ma et al. (2018) tested seven built up I-section columns, as shown in Table 1. These columns were fabricated using HS3 plate with a yield strength of 690 MPa (100 ksi). Four different I-sections were considered with two different effective lengths. All of the columns were concentrically loaded with pinned-pinned end conditions. In addition to providing dimensional information for each column, Table 1 also reports column capacity obtained from the experimental results, P_{exp}.

The same geometric properties, loading, and end conditions from the experimental study were used to model the columns in ABAQUS. Initial geometric imperfections were incorporated as reported by Ma et al. (2018). Residual stresses were not assigned to the FEM model. In the experimental evaluation, all columns failed in flexural buckling and no weld failures were reported. Thus, the welds were not explicitly modeled but were idealized as a tie constraint between the plates. The load was applied concentrically at the geometric centroids of all cross-sections. Table 1 shows the load-carrying capacity for each column as determined from the finite element analysis, P_{FEM}. The failure mode of all columns analyzed by ABAQUS was weak-axis flexural buckling, as observed in the experiment. The load-carrying capacity determined from FEM and the experimental study were compared as a ratio, P_{FEM}/P_{exp}. Among the seven tests, the mean value of P_{FEM}/P_{exp} was found to be 1.01 with a coefficient of variation of 9.2% and a standard deviation of approximately 0.092, which shows that the numerical model can adequately predict the load capacity of high strength structural steel.

Table 1: Column capacity as determined by experiment and ABAQUS.

Specimen	Column size (mm x mm)	Flange Thickness (mm)	Web Thickness (mm)	Length (mm)	$P_{exp.}$ (kN)	P_{FEM} (kN)	$P_{FEM}/P_{exp.}$
CH1P	W120x120	10.0	6.0	1995	1284	1306	1.017
CH2P	W150x150	10.0	6.0	1995	2714	2430	0.895
CH2Q	W150x150	10.0	6.0	2794	1510	1291	0.855
CH3P	W200x200	16.0	10.0	1995	5924	6668	1.126
CH3Q	W200x200	16.0	10.0	2794	4644	5099	1.01
CH4P	W250x250	16.0	10.0	1995	7739	8033	1.038
CH4Q	W250x250	16.0	10.0	2794	7284	7580	1.041
Mean							1.01
COV							9.2%

4. Parametric Studies

After validation of the modeling approach, a parametric study was conducted to evaluate two column sizes, four different yield strengths, and four different slenderness ratios. Table 2 shows these parameters that were evaluated in order to determine the load-carrying capacity of W12×58 and W14×90 columns. These two column sizes were selected because they are common sizes used for gravity columns and are compact shapes. HS3 columns with 550 MPa (80 ksi), 690 MPa (100 ksi), and 890 MPa (130 ksi) yield strengths were considered. Conventional steel with a yield strength of 350 MPa (50 ksi) was also considered for comparison.

Twenty-four analyses were conducted to encompass these different parameters. The slenderness ratio is the ratio of the effective length of the column relative to the radius of gyration about the weak axis. A slenderness ratio of 40 represents columns with lengths approximately equal to 2.6 m (8.5 ft) and 3.7 m (12 ft) for W12×58 and W14×90 shapes, respectively. A W12×58 column with 160 slenderness is about 10 m (33 ft) long and a W14×90 column with the same slenderness is about 15 m (50 ft) long. All of the columns failed into flexural buckling, as shown in Figure 5. It is acknowledged that columns with unbraced lengths of 2.6 m (8.5 ft) and 15 m (50 ft) are atypical for building construction, but they were evaluated in order to evaluate the effect of column slenderness on column behavior. Figure 5: Buckling failure of W12×58 column with 40 slenderness for 690 MPa yield strength by RIKS

Table 2: Parameters for column capacity

W-Shapes	Yield Strength MPa (ksi)	Slenderness
W12×58	350 (50)	40
W14×90	550 (80)	80
	690 (100)	120
	890 (130)	160

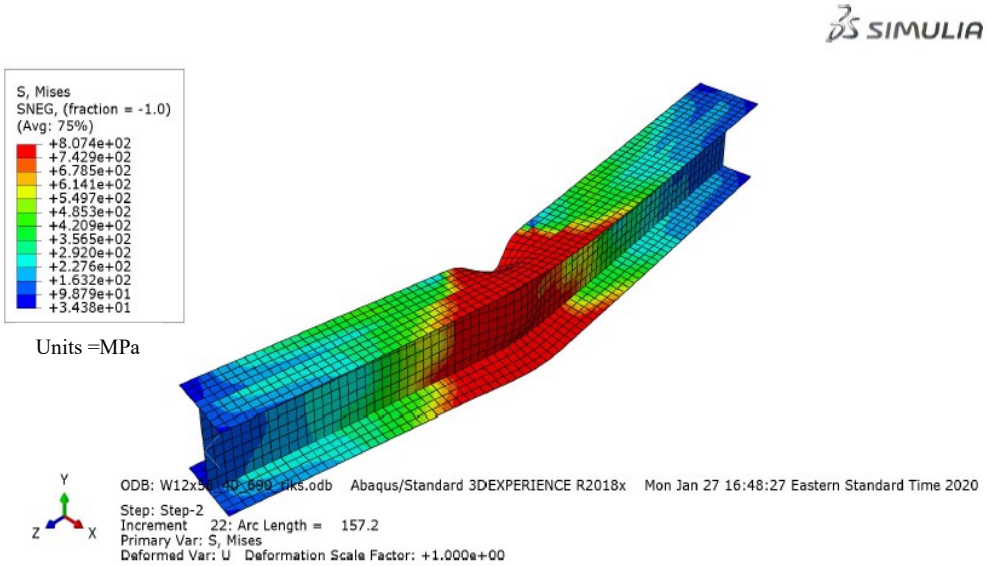

Figure 5: Buckling failure of W12×58 column with 40 slenderness for 690 MPa yield strength by RIKS analysis.

4.1 Results and Discussion

Figure 6 shows the load carrying capacity with respect to column slenderness for each of the HS3 gravity columns analyzed in the parametric study using the FEM model. It can be seen from the graph plotted that the gravity column with highest yield strength shows the highest capacity and the lowest capacity is shown by the lowest yield strength amongst three HS3 steel. The overall capacity of HS3 columns decreases with increasing slenderness with the highest difference shown at 40 slenderness and becoming almost equal at higher slenderness, i.e., 120 or 160. This behavior of the HS3 column is due to fact that at low slenderness the column's capacity is governed by the yield strength and a higher slenderness column's strength is governed by elastic modulus or stiffness, which is same for all three HS3 steel. The same conclusion was made by Agarwal (2011)

for mild steel gravity column. This shows that HS3 gravity column display similar behavior to mild steel in regards to slenderness.

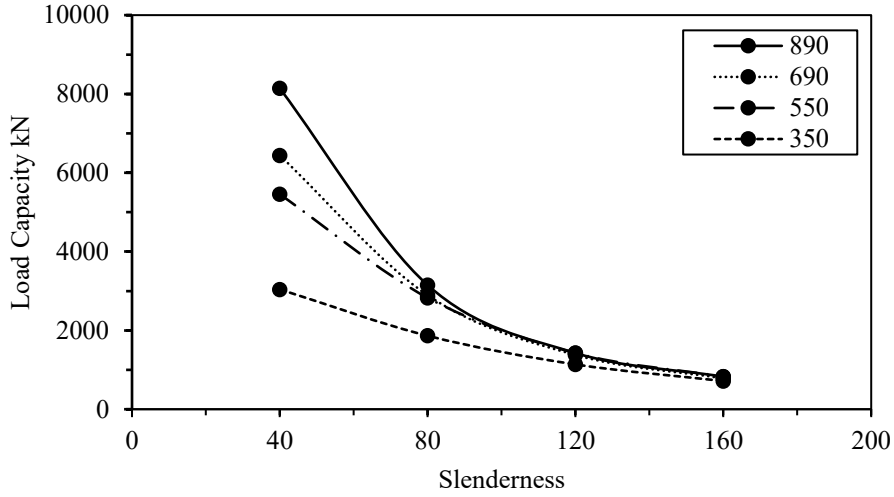

(a) W12×58

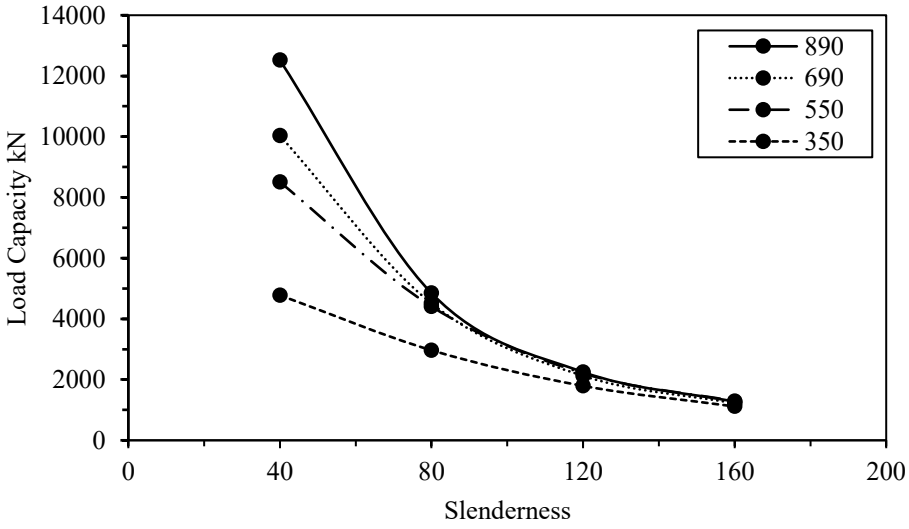

(b) W14×90

Figure 6: Load carrying capacity of HS3 columns and comparison with conventional steel.

Figure 6 also shows the load carrying capacity of conventional 350 MPa (50 ksi) steel columns relative to HS3 columns. The same numerical approach described for HS3 steel column analysis was used to determine the conventional steel column strengths. In general, HS3 gravity columns show higher capacity in comparison to conventional steel with the largest difference at the 40 slenderness and minimal differences at higher slenderness. This is again due the differences in modes of failure; stub columns are more influenced by inelastic buckling which is affected by

yield strength and slender columns are more prone to elastic buckling which is affected by material stiffness. Similar behavior was observed for both W12×58 and W14×90 sections.

Although the W14×90 shows higher capacity in comparison to W12×58, the same percentage difference was observed at all slenderness levels. The load-carrying capacity of W14×90 was approximately 1.5 times the capacity of W12×58 for all slenderness levels. This higher load-carrying capacity of W14×90 can be attributed to its larger cross-sectional area and higher moment of inertia in comparison to W12×58. This comparison shows that there is no significant difference in the behavior of HS3 gravity column between W12×58 and W14×90. However, very lightweight (i.e. slender) and very heavy (i.e. jumbo) column shapes are expected to exhibit behavioral differences.

Figure 7 shows the percentage increase in the capacity of HS3 steel gravity columns with respect to convention 350 MPa (50 ksi) steel at different slenderness ratios for W14×90. It can be seen from the graph that HS3 steel shows significantly higher capacity ranging from about 80% to more than 160% than conventional steel for the slenderness of 40. An increase of approximately 50 to 60% of the capacity was also observed at the slenderness of 80. The increase in capacity is less than 20% at the higher slenderness ratios of 120 and 160.

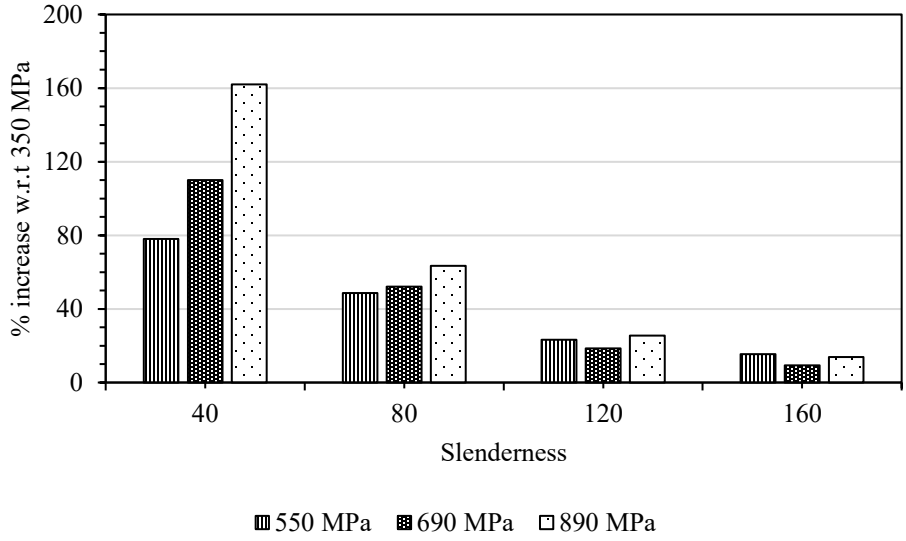

Figure 7: Percentage increase in load capacity of W14×90 HS3 w.r.t Conventional W14×90 Column

It can be concluded from the load carrying capacity comparison of HS3 gravity column with mild steel gravity column that HS3 gravity columns result in higher capacities than conventional steel columns; thus, smaller cross-sections may be able to be used in HS3 designs, likely meaning less material. However, the benefits of HS3 are minimal when considering higher slenderness levels (i.e. 120 and 160).

5. Evaluation of AISC Equations

The applicability of flexural buckling design equations from the AISC *Specification* (2016) for design of HS3 columns were evaluated in this section. Flexural buckling of compressive members without slender elements is defined in Section E3 of the *Specification*. This design is based on a

single column curve that differentiates elastic and inelastic buckling. The critical stress, F_{cr}, is evaluated based on the slenderness of the column. The nominal compressive strength, P_n, in less slender columns are controlled by yield strength, F_y, while more slender columns are controlled by the elastic buckling stress, F_e, as shown in the design equations E3-1 through E3-4 from the *Specification* reproduced below:

$$P_n = F_{cr} A_g \tag{1}$$

where A_g is the gross cross-sectional area of the member.

$$F_{cr} = \left(0.658^{F_y/F_e}\right) F_y \tag{2}$$

$$F_{cr} = 0.877 F_e \tag{3}$$

$$F_e = \frac{\pi^2 E}{\left(\frac{L_c}{r}\right)^2} \tag{4}$$

where L_c is the effective length of the member, r is the radius of gyration, and E is the modulus of elasticity.

These design equations were directly applied to the HS3 columns using the material properties provided in Huang et al. (2018). The nominal compressive capacity was calculated for each column from the parametric study. The results for the W14×90 HS3 columns and are presented in Fig. 8 for each yield strength. "ABAQUS" represents the results obtained from the FEM study, while "AISC" represents the nominal capacity calculated using the AISC *Specification* (2016). It can be seen from the results presented that the AISC equations predicted the load capacity of the HS3 column with reasonable accuracy. The maximum error is only approximately 10%. A more thorough analysis is needed to evaluate the reliability of this procedure and whether the resistance factor of 0.9 used with conventional steel is appropriate.

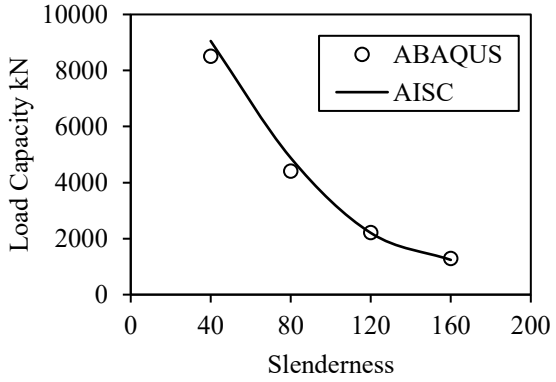

a) 550 MPa

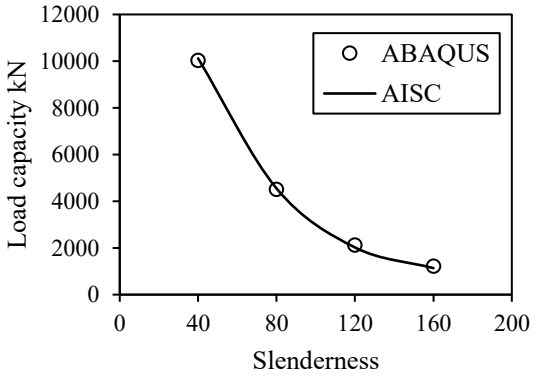

b) 690 MPa

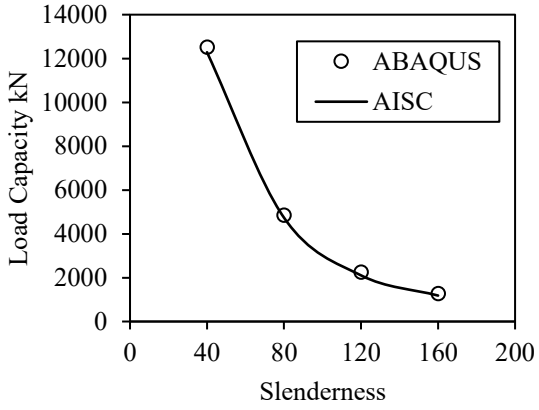

c) 890 MPa

Figure 8: Comparison of load capacity of HS3 gravity from ABAQUS and AISC equation for W14×90

6. Conclusion

A numerical evaluation of high strength structural steel was conducted in order to evaluate the potential benefits of using HS3 gravity columns in building construction. Benchmarking of the numerical modeling was performed against the experimental evaluation performed by Ma et al. (2018). In the parametric study, the load-carrying capacity of HS3 gravity columns (W12×58 and W14×90) was determined for three yield strengths of 550 MPa, 690 MPa, and 890 MPa and four slenderness ratios: 40, 80, 120, and 160. The results of the numerical analysis were also compared with conventional steel columns to evaluate the increased strength of HS3 gravity columns over traditional gravity columns. Applicability of current AISC equations to predict the buckling capacity of columns was also evaluated.

Based on the numerical investigation conducted in this study, the following conclusions can be drawn:

- The load carrying capacity of the HS3 gravity columns increased with yield strength for shorter columns, but remain essentially unchanged for slender columns. Thus, there is a clear advantage of using HS3 gravity columns for short columns. Longer columns, however, are less influenced by increased yield strength because these columns are more controlled by elastic buckling, which is dictated by the modulus of elasticity that remains unchanged for all steel types.
- The load-carrying capacities of the HS3 gravity columns was higher than the capacities determined from the conventional steel columns. An increase of 80-160% was exhibited at the slenderness of 40 and about 20% increase was shown at slenderness ratios of 120 and 160.
- Current AISC equations used to predict the flexural buckling capacity of gravity columns were found to be applicable for HS3 gravity columns. The nominal capacity determined from these equations can predict HS3 capacities within 10%.

Additional work is needed to expand the parametric study and evaluate other column sizes. This includes determination of local slenderness limits and evaluating the effects of local buckling. Experimental studies should also be performed to better quantify typical residual stress profiles in

HS3 cross-sections. Further, experimental testing of rolled shapes are needed, as much of the previous work focused on built-up sections which likely experience different residual stresses and imperfections. Evaluation of HS3 columns under fire conditions is also needed. A future publication is underway by the authors of this paper that will address the behavior of these columns under elevated temperatures.

References

ABAQUS (2016), Simulia - Dassault Systemes, Boston, Mass.

AISC, (1993). "Load and Resistance Factor Design Specification for Structural Steel Buildings." *American Institute of Steel Construction*, Chicago, Ill.

AISC, (2016). "ANSI/AISC 360-16: Specification for Structural Steel Buildings." *American Institute of Steel Construction,* Chicago, Ill.

AISC Committee on Specification, (2019). "High strength steel." *American Institute of Steel Construction,* Chicago, Ill. (Issue 21 November).

Agarwal, A. (2011). "Stability Behavior of Steel Building Structures in Fire Conditions," *Doctoral Dissertation*, School of Civil Engineering, Purdue University, West Lafayette, Ind

American Society of Testing and Materials, (2019). *ASTM A6 / A6M - 19: Standard Specification for General Requirements for Rolled Structural Steel Bars, Plates, Shapes, and Sheet Piling*.

Australian Standard. (1990). "AS 4100-1990: Steel Structure." *Australian Building Code Board*, Sydney.

Baddoo, N., & Brown, D. (2015, September). "High Strength Steel." *New Steel Construction*.

Ban, H., Shi, G., Shi, Y., & Bradford, M. A. (2013). "Experimental investigation of the overall buckling behaviour of 960 MPa high strength steel columns." *Journal of Constructional Steel Research*, *88*, 256–266. https://doi.org/10.1016/j.jcsr.2013.05.015

British Standards Institution. (1990). BS 5950-1; Structural use of steelwork in building; Part 1: Code of practice for design in simple and continuous construction: hot rolled sections; (pp. 1–153).

European Committee for Standardisation. (1992). *Eurocode 3: Design of steel structures - Part 1-1: General rules and rules for buildings*.

European Committee for Standardization. (2011). *Eurocode 3: Design of steel structures - Part 1-1: General rules and rules for buildings* (Vol. 1, Issue 2005).

Huang, L., Li, G. Q., Wang, X. X., Zhang, C., Choe, L., & Engelhardt, M. (2018). "High Temperature Mechanical Properties of High Strength Structural Steels Q550, Q690 and Q890." *Fire Technology*, *54*(6), 1609–1628. https://doi.org/10.1007/s10694-018-0760-9

Kim, D. K., Lee, C. H., Han, K. H., Kim, J. H., Lee, S. E., & Sim, H. B. (2014). "Strength and residual stress evaluation of stub columns fabricated from 800 MPa high-strength steel." *Journal of Constructional Steel Research*, *102*, 111–120. https://doi.org/10.1016/j.jcsr.2014.07.007

Ma, T. Y., Liu, X., Hu, Y. F., Chung, K. F., & Li, G. Q. (2018). "Structural behaviour of slender columns of high strength S690 steel welded H-sections under compression." *Engineering Structures*, *157*(December 2017), 75–85. https://doi.org/10.1016/j.engstruct.2017.12.006

National Standard of the People's Republic of China. (2009). *GB 50017-2003: Code for Design of Steel Structure* (Issue January, pp. 1–22).

Oakley, D. (2014). "Examples and Applications of High Strength Steel." Oakley Steel. https://www.oakleysteel.co.uk/examples-applications-high-strength-steel#comments

Rakshe, B., & Patel, J. (2010). "Modern high strength Nb-bearing structural steels." *Millennium Steel India*, 69–72.

Rasmussen, K., & Hancock, G. J. (1995). "Tests of High Strength Steel Columns." *Journal of Constructional Steel Research*, *34*(1995), 27–52.

Somodi, B., & Kövesdi, B. (2018). "Residual stress measurements on welded square box sections using steel grades of S235–S960." *Thin-Walled Structures*, *123*(July 2016), 142–154. https://doi.org/10.1016/j.tws.2017.11.028

Takagi, J., & Deierlein, G. G. (2007). "Collapse Performance Assessment of Steel-Framed Building Under Fire." *The John A. Blume Earthquake Engineering Centre, Stanford University*, *March*.

Uy, B. (2001). "Strength of short concrete filled high strength steel box columns." *Journal of Constructional Steel Research*, *57*(2), 113–134. https://doi.org/10.1016/S0143-974X(00)00014-6